Proc. 1st International Conference on
Mineral Engineering and Materials Science (iCMEMS2017)
20-22 Nov 2017, Sydney, Australia
ISBN: 978-0-6480147-7-5

Effects of Codopant (Co + V) Concentration and Distribution on the Photocatalytic Properties of Sol-Gel-Derived TiO_2 Thin Films

[1]Wen-Fan Chen, [1]Gustad Irani, [2]Rong Liu, [1]Charles C. Sorrell, [1]Pramod Koshy

[1]School of Materials Science and Engineering, UNSW Sydney NSW 2052 Australia
[2]Secondary Ion Mass Spectrometry Facility, Office of the Deputy Vice-Chancellor (R&D), Western Sydney University, Penrith, NSW 2751, Australia
Corresponding author's E-mail: w.chen@unsw.edu.au

Abstract

The type, concentration, and distribution of dopants in TiO_2 thin films have a huge impact on their photocatalytic performance. In the present work, spin coating followed by annealing at 450°C for 2 h in air, was utilised to fabricate TiO_2 thin films codoped with V and Co (0.02-2.00 mol% total codopant concentration) on fused silica substrates. Two unique codoped TiO_2 thin films with varying through-thickness dopant concentration were fabricated in addition to the samples with a conventional constant concentration throughout the film. One film had a descending concentration (DC) of codopants from the film surface to the substrate-film interface, while the other had an ascending concentration (AC) of codopants from the film surface to the substrate-film interface. GAXRD and Raman analysis confirmed that all fabricated films were composed of anatase and the data suggested that that the dopants were incorporated into the lattice. AFM analysis showed that the grains were small and uniform for all the films and did not change with the codopant concentration. At higher codopant concentrations, surface amorphisation and liquid formation occurred which led to a reduction in surface roughness and crystallinity; in addition, pores were also formed on the surface. SIMS analysis confirmed the varying distribution levels in the AC and DC films and the constant levels in the other films. XPS analysis identified the presence of Co^{2+}, Co^{3+}, V^{3+}, V^{4+}, and possibly V^{5+} suggesting the presence of intervalence charge transfer. UV-Vis analysis showed that the films were highly transparent (~80%) in visible light with similar band gap values. Assessment of photocatalytic performance in terms of methylene blue degradation showed that the DC sample outperformed the AC sample due to its greater roughness, larger grain size, higher crystallinity and smaller band gap.

Keywords: Codoping, Dopant Distribution, TiO_2 Thin Film, Sol-Gel

1. INTRODUCTION

Titania (TiO_2) is the most popular photocatalyst owing to its superior stability and low costs. Titania exists mostly as anatase and rutile (**Ren et al 2017)**. Rutile has a lower band gap compared to anatase; anatase is generally present in smaller grain sizes and has greater electron-hole recombination times and this contributes to this phase possessing superior photocatalytic activity **(Torimoto et al 2000, Hanaor and Sorrell 2012)**. However, both anatase and rutile have high bad gap values (3.0-3.2 eV); this implies that radiation with wavelengths less than 400 nm (*i.e.* UV) is required for photocatalytic activation which leads to poor efficiencies in sunlight. Titania can be fabricated in the form of particles and films. Particles have higher efficiencies compared to films; however films have greater lifetimes of usage and can be more effectively utilised in surface coatings. Recent research has focussed largely on enhancing the potential for activation of titanium dioxide using visible light and the strategies used have focussed on reducing the band gap by introducing intermediate band gap states by doping. Transition metal doping has been seen to result in a significant red shift (i.e. increased visible light absorption) in the absorption spectrum. Further, codoping is another strategy where two or more dopants are added together to generate a synergistic effect to improve the

photocatalytic effect. Recently codoping has been researched because of the attraction of the synergistic effect on tuning the electronic structure and enhancing the visible-light photo activity **(Lin et al 2014, Xiang et al 2011)**. **Hamal et al (2011)** fabricated 2 mol% Co/(C,S)-TiO_2 nanoparticles to study their performance under visible light. **Chen et al (2015)** prepared codoped thin film samples of Co-V-TiO_2 via spin coating of a sol-gel and showed that the 0.05 mol% Co + 0.05 mol% V sample had the best performance. Intervalence charge transfer was observed in higher concentration samples, inducing lattice strain, decreasing the photocatalytic performance. However, this work involved the use of films with constant distribution of dopants and codopants in their structure.

The effect of creating a film with such a distribution of concentration may be extrapolated from the results of **Yasumori et al (1998)** who deposited a SiO_2 film onto an Al_2O_3 substrate, followed by a platinum film and then a thin film of TiO_2. This form of multilayer deposition created a charge potential between layers, allowing for charge separation. Therefore, the present work investigates the effects of codopant (Co + V) concentration and distribution on the mineralogical, morphological, optical and chemical characteristics of the films in order to determine the effects of these parameters on the photocatalytic properties of the films.

2. EXPERIMENTAL

2.1 Sample Preparation

Thin films of nine codopant concentrations were fabricated for testing. The precursor solutions were prepared by mixing titanium tetra-isopropoxide (TTIP, Reagent grade, 97 wt%, Sigma Aldrich), isopropanol (Reagent Plus, 99 wt%, Sigma- Aldrich) with $CoCl_2$ (Reagent Grade, 97 wt%, Sigma-Aldrich) and VCl_3 (≥99 wt% purity, Sigma-Aldrich). The resulting 100 mL solutions were magnetically stirred in a borosilicate beaker placed on a stirring/heating plate (Barnstead, Thermolyne Mirak) for 5 min at 65°C at 200 rpm. Seven sets of films were fabricated with a uniform distribution of codopants in the following amounts: 0.00, 0.01, 0.05, 0.10, 0.20, 0.40, and 1.00 mol% (metal basis). Two sets of films were fabricated with either an ascending (AC) or descending (DC) dopant concentration from the top to the bottom of the film. Fused silica substrates were coated using the precursor solution with a spin coater (Laurell, WS-650SZ-6NPP). 0.2 mL (10 drops) was deposited onto the spinning substrate in the first 10 s; the speed was increased to 2,000 rpm and held for 13 s; after this, the speed was reduced to zero. The sample was dry on a 65°C hot plate for 5 min before loading back into the spin coater for the next layer. This process was repeated to fabricate thin film samples with seven layers of undoped or codoped TiO_2.

2.2 Glancing Angle X-Ray Diffraction

Glancing angle XRD was used to analyse the minerology of the films and was done using an XRD unit (PANalytical, Empyrean; range of 20° to 80° 2θ; step size of 0.026° 2θ). The scan was done with 40 mA and 45 kV as the generator settings.

2.3 Atomic Force Microscopy

PeakForce Tapping^{TM} mode on an AFM unit (Bruker) was used to measure a 1 μm^2 area with a cantilever with 0.4 N/m spring constant to determine the topologies. The scan rate was set to 0.501 Hz and the resolution was 512 samples per line.

2.4 Secondary Ion Mass Spectrometry

A SIMS unit (Cameca, IMS 5fE7) was used to determine the elemental distribution through the thickness and this was done using a primary ion beam of O_2^+, with an impact energy of 7.5 keV and beam current of 60 nA, to raster a 180 x 180 μm region. To run the analysis, a gold film was deposited onto the sample surface using a sputter coater (Leica, EM S5).

2.5 Ultra Violet - Visible Spectrophotometry

A UV-Vis spectrometer (PerkinElmer, Lambda 35) was used to determine the film transmittance over a 300-800 nm wavelength range in standard transmission mode. A scan speed of 480 nm/min with a 1 nm data interval ensured a high resolution scan. Band gap energy calculations were done using the absorption characteristics. Standard absorption mode was run with the same operating parameters as standard transmission mode on the UV-Vis Spectrometer.

2.6 X-Ray Photoelectron Spectroscopy

XPS was chosen to analyse the surface composition (Ti, O, V, Co and Si) for all the films and this was done using a Thermo Scientific, ESCALAB 250Xi with 13.8 kV and 8.7 mA to analyse the sample surface at a depth of 2-5 nm; the beam dimension was 500 μm in diameter.

2.7 Photocatalytic Activity

The photocatalytic activity of all samples was compared by measuring the extent of photo-bleaching of a methylene blue (MB) solution. Methylene blue (M9140, dye content ≥82 wt%, Sigma-Aldrich) and deionised water were mixed to prepare a 10^{-5} M MB solution. Mixing was done using magnetic stirring (Barnstead, Thermolyne Mirak). The thin film samples were submerged in the MB solution and kept in a sealed opaque container for 24 h. The films were then submerged in fresh MB solution and exposed to UV light for 8, 12, and 24 h using an overhead UV lamp (UVP, 3UV-38) in a light obstructing container. Immediately after the irradiation time was completed, part of the degraded solution was extracted and its absorbance was measured using UV-Vis spectrophotometry.

3. RESULTS AND DISCUSSION

Figure 1 shows the GAXRD patterns for all the TiO_2 films with varying codopant levels. Anatase was the only crystalline phase observed in all the samples. The peak intensity appeared to increase with increasing total codopant level to 0.02 mol% (0.01 mol% Co + 0.01 mol% V), after which the intensities were stable up to a total codopant level of 0.8 mol% (0.04 mol% Co + 0.04 mol% V). With further increase in the codopant concentrations, the intensities appeared to decrease. DC and AC had very similar crystallinity, showing that orientation of doping did not affect crystallography.

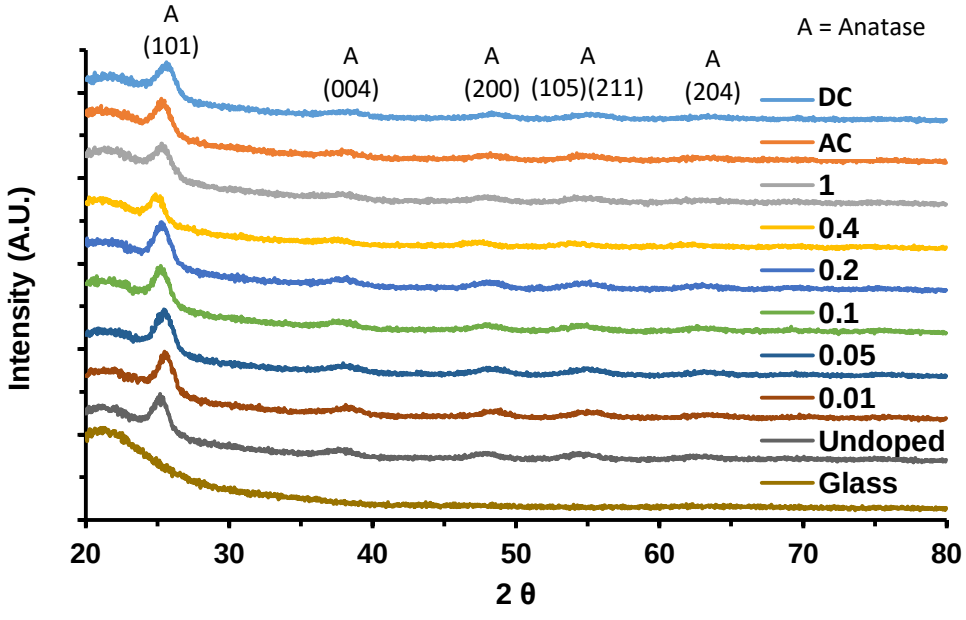

Figure 1. ***XRD patterns of the codoped TiO_2 thin films***

At low codopant concentrations (0.02-0.10 mol% total), the dopants were observed to be incorporated in the anatase lattice leading to a reduction of the lattice spacing owing to oxygen vacancy formation. At low codopant concentrations, dopant incorporation in the lattice created defects owing to solid solution formation, thereby assisting recrystallisation and increasing the overall crystallinity. At 0.20 mol% total codopant concentration, the solubility limit was reached, resulting in precipitation at the grain boundaries and lowering of crystallinity. At 0.40 mol% total codopant concentration, the crystallinity increased, suggesting that intervalence charge transfer may have occurred to form the more thermodynamically favourable V^{5+} ion, leading to the formation of Ti-interstitials, which would again contribute to anatase recrystallisation. Crystallinity decreases with increase in codopant concentrations resulting in V^{5+} reaching its solubility limit and excess dopants were being precipitated on the grain boundary, leading to surface amorphisation and reduction in crystallinity.

AFM analysis results (**Figure 2**) showed that the roughness increased with increasing codopant concentration up until 0.20 mol% total concentration, and then decreased. The grain sizes were similar for all codopant concentrations in general (except the 0.10 mol% V + 0.10 mol% Co sample) which showed slightly larger size for the grains. This sample also showed the highest roughness. This data suggests that the grain growth and recrystallisation enhanced surface roughness. Liquid formation at higher codopant concentrations was observed to cause an increase in the occurrence of pores on the surface; the size of the pores increased with increasing codopant concentration, confirming that precipitation of the codopants occurred on the grain boundaries at higher codopant concentrations and this was responsible for the amorphisation and liquid formation. The AC sample had a surface grain structure similar to that of the undoped sample, which is probably due to the DC sample having an undoped layer at its surface. The DC sample had a larger grain size and surface roughness suggesting the orientation of codopant distribution has an effect on grain sizes.

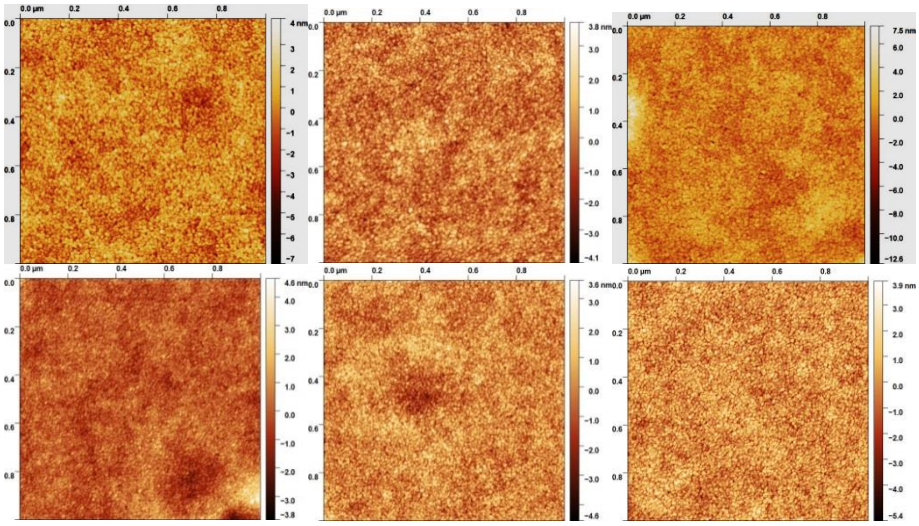

Figure 2. ***AFM images of the undoped, 0.01 mol% V + 0.01 mol% Co, 0.10 mol% V + 0.10 mol% (top - left to right) Co, 1.00 mol% V + 1.00 mol% Co, AC and DC codoped TiO_2 thin films (bottom – left to right)***

UV-Vis analysis results (not shown here) showed that all the films had reasonably high absorption values in the UV regions and high transmittance in the visible region. The band gap energy decreased at the very low codopant concentrations and then increased with increasing codopant concentrations. The DC sample, with its highest concentration at the surface, showed a significantly lower band gap energy, suggesting the distribution of codopants affects the formation of mid-gap states and enhances electron-hole separation through the use of a graded concentration layer.

SIMS analysis was able to reveal that the distributions of the codopants were uniform and constant throughout the thickness in the single concentration films. In the AC and DC films, the concentrations were in the expected distribution profile as shown in **Figure 3** (for the AC film).

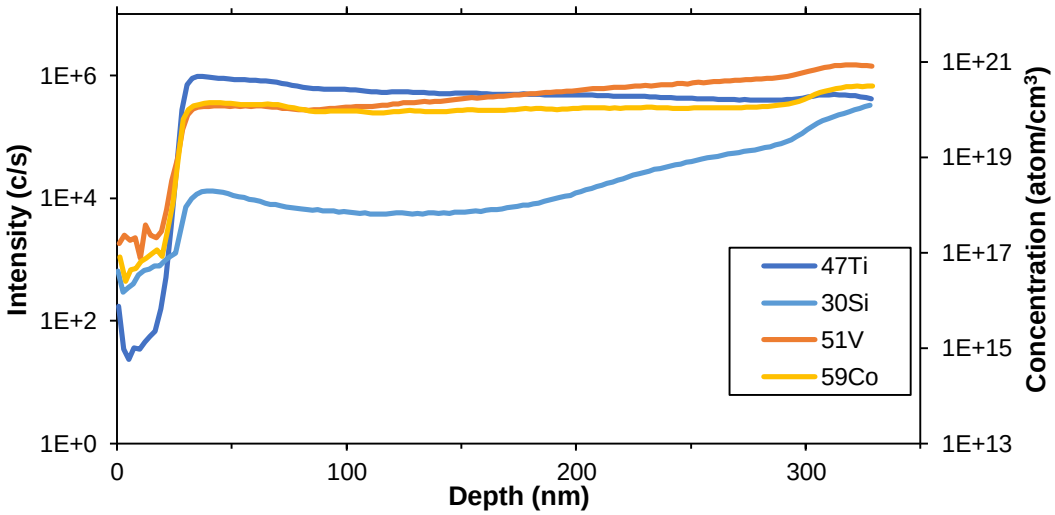

Figure 3. ***SIMS analysis data for AC codoped TiO_2 thin films***

XPS analysis (not shown here) showed that Co^{2+}, Co^{3+}, V^{3+} and V^{4+} (and possibly V^{5+}) were present in the samples due to the presence of the starting dopant valence states, thermodynamic considerations, and intervalence charge transfer. The Ti binding energies for the AC and DC films were higher than any of the constant concentration samples. This could be owing to the distribution being able to assist in incorporating both dopants into the lattice to create a unique bonding configuration which is energetically more favourable.

The photocatalytic properties of the films are shown in **Figure 4**. The undoped film, and the two lowest concentrations of codopants consistently performed the best at shorter irradiation times (8 and 12 h) while the undoped, three lowest codopant concentrations and DC sample showed similarly good performances at 24 h of irradiation. The DC sample showed a constant improvement in performance with increasing irradiation time and had a relatively good performance value for the 24 h test. The AC specimen had similar 8 h and 12 h performance to the DC sample, but did not perform as well when compared at 24 h irradiation. The DC and AC samples showed performances that were similar for 8 and 12 h UV irradiation times, but the DC sample showed a significantly better performance for the 24 h test.

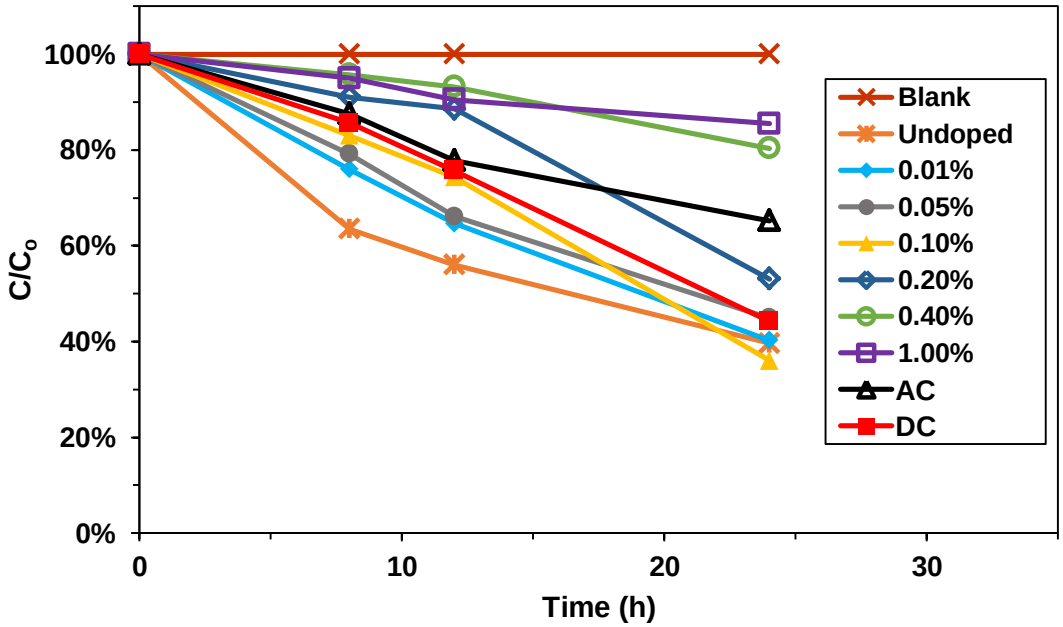

Figure 4. ***Photocatalytic performance of the codoped TiO_2 thin films***

4. CONCLUSIONS

All the films showed the presence of anatase as the sole crystalline phase; the films were also highly transparent in the visible region. The grain sizes did not show any major differences with variations in the codopant concentration. The best photocatalytic performance was seen in the films with lower codopant concentrations owing to the combination of several factors including the higher crystallinity, greater grain size and higher surface roughness, lower band gap energies. The reason for these effects is related to dopant incorporation into the anatase lattice at the very low levels which results in defect formation thereby altering the crystallinity and the electronic structure.

In the AC and DC samples, anatase was again the sole crystalline phase and the distribution of codopants did not affect the crystallinity. However, there were minor differences in the surface roughness. Moreover, the bonding energies for Ti-O were observed to shift to higher values for the samples with the varying dopant distributions in comparison with those films with the constant distribution. Moreover, the former films showed slightly lower band gap energies. This shows that the dopant distribution can alter the electronic structure and modify electron-hole recombination behaviour.

ACKNOWLEDGEMENTS

We acknowledge the funding provided by the ARC-Discovery project as well as the access to the analytical facilities at the Mark Wainwright Analytical Centre UNSW Sydney.

REFERENCES

[1] Ren H, Koshy P, Chen W-F, Qi S, Sorrell CC, (2016), Photocatalytic materials and technologies for air purification. Journal of Hazardous Materials 325, 340–366.
[2] Torimoto T, Nakamura N, Ikeda S, Ohtani B, (2002), Discrimination of the active crystalline phases in anatase-rutile mixed Titanium(iv) oxide photocatalysts through action spectrum analyses, Physical Chemistry Chemical Physics 4 [23] 5910-5914.
[3] Hanaor DAH and Sorrell CC, (2011) Review of the anatase to rutile phase transformation, Journal of Materials Science 46 [4] 855-874.
[4] Lin MZ, Chen H, Chen WF, Nakaruk A, Koshy P, Sorrell CC, (2014), Effect of single-cation doping and codoping with Mn and Fe on the photocatalytic performance of TiO_2 thin films, International Journal of Hydrogen Energy 39 [36] 21500-21511.
[5] Xiang Q, Yu J, Jaroniec M, (2011) Nitrogen and sulfur co-doped TiO_2 nanosheets with exposed {001} facets: synthesis, characterization and visible-light photocatalytic activity, Physical Chemistry Chemical Physics. 13 [11], 4853-4861.
[6] Chen WF, Koshy P, Sorrell CC, (2015), Effect of intervalence charge transfer on photocatalytic performance of cobalt- and vanadium-codoped TiO_2 thin films, International Journal of Hydrogen 40 [46] 16215-16229.
[7] Hamal DB and Klabunde KJ, (2011),Valence state and catalytic role of cobalt ions in cobalt TiO_2 nanoparticle photocatalysts for acetaldehyde degradation under visible light, Journal of Physical Chemistry C 115 [35] 17359-17367.
[8] Yasumori A, Ishizu K, Hayashi S, Okada K, (1998), Preparation of a TiO_2 based multiple layer thin film photocatalyst, Journal of Materials Chemistry 8 [11] 2521-2524..